J Mater Sci (2011) 46:7262–7274
DOI 10.1007/s10853-011-5686-2

Isothermal aging effect on the microstructure and dry sliding wear behavior of Co–28Cr–5Mo–0.3C alloy

H. R. Lashgari · Sh. Zangeneh · M. Ketabchi

Received: 28 March 2011 / Accepted: 2 June 2011 / Published online: 21 June 2011

Abstract In this study, an attempt to investigate the role of isothermal aging on the microstructure and dry sliding wear behavior of Co–28Cr–5Mo–0.3C alloy was made. Regarding the results, it is clear that isothermal aging at 850 °C for 8 and 16 h contributed to the formation of lamellar type carbides (γ-fcc + $M_{23}C_6$) at the grain boundary regions. Moreover, at higher aging times (24 h), the lamellar type carbides decreased whereas severe precipitation of carbides was found to occur on the stacking faults. Furthermore, according to X-ray diffraction results, 24 h isothermal aging of solution treated specimens did not lead to complete fcc → hcp transformation. The wear properties of as-cast and heat treated samples were determined at 0.5 ms^{-1} speed several under normal applied loads such as 50, 80, and 110 N. At the lowest load applied (50 N), isothermally aged specimens for 8 and 16 h have higher wear resistance probably due to more volume fraction of lamellar-type carbides when compared to as-cast for both 4 and 24 h aged specimens. But, at higher applied loads (80 and 110 N) due to the formation of adhesive oxide layer on the as-cast specimen surface, the wear rate of as-cast samples is lower compared with all heat treated specimens.

H. R. Lashgari (✉)
Center of Excellence for High Performance Materials, School of Metallurgy and Materials Science, University of Tehran, Tehran, Iran
e-mail: hrlashgari@ut.ac.ir

Sh. Zangeneh · M. Ketabchi
Department of Mining and Metallurgical Engineering, Amirkabir University of Technology, Tehran, Iran

Introduction

ASTM F75 cast alloy, with a Co–28Cr–5Mo–0.3C nominal wt% composition, is one of the most widely used cobalt-base alloys for orthopedic implants such as knee, hip, and shoulder [1–3]. It is well-known that in the as-cast condition, a decrease in the mechanical properties can be expected due to inhomogeneities in carbide morphology, size, and distribution [4]. Conducting heat treatments in Co-base alloys contribute to the elimination of primary segregation and formation of various microstructural features including stacking faults, twins, and uniform distribution and precipitation of carbide those features can affect the final properties of the alloy particularly wear behavior.

In previous works [5, 6], the role of heat treatment process on the microstructural evolution of Co–28Cr–5Mo–0.3C was investigated and reviewed in this work. The aim of this study is to investigate the effect of isothermal aging at 850 °C for various times (4, 8, 16, and 24 h) on the dry sliding wear behavior in order to point out how microstructural features influence the final wear properties of a Co–28Cr–5Mo–0.3C alloy.

Experimental procedure

Table 1 summarizes the chemical composition of as-cast cobalt-base alloy used in this investigation. The as-cast specimens were subjected to a solution thermal treatment at 1230 ± 5 °C for 3 h in a tubular furnace with an argon controlled atmosphere and finally quenched in cold water. Following this, all specimens were aged at 850 °C for 4, 8, 16, and 24 h.

For microstructural studies, all specimens were polished up to mirror-like surface and etched with a reagent containing 92 pct HCl, 5 pct H_2SO_4, and 3 pct HNO_3. Moreover,

Table 1 Chemical composition of cobalt alloy (wt%)

%Cr	%Mo	%C	%Si	%Co
28	5	0.3	1.5	Rem.

the microstructures were analyzed by using optical (OM) and scanning electron microscopy (SEM) equipped with a energy dispersive X-ray spectrometer (EDS). Phase identification was carried out by X-ray diffraction method by using Cu Kα ($k = 1.54184$ Å) radiation in a Philips machine. The scan angle (2θ) was selected between 40° and 55° with step size of 0.02° $2\theta \times S^{-1}$. The X-ray diffraction experiments were employed for determinations of the most intense isolated $(200)_{fcc}$ and $(10\bar{1}1)_{hcp}$ X-ray diffraction peaks [7]. Also, the phase transformation effect on the microhardness of Co–28Cr–5Mo–0.3C was determined by using a microdurometer with a $L = 50$ g load. For each specimen, at least five points were measured for microhardness test.

Wear testing were conducted on a conventional pin-on-disk testing machine at room temperature to determine the wear behavior of as-cast and heat-treated specimens sliding against 100Cr6 steel disk with a hardness of 62HRC according to ASTM G-99. The pins were machined down to become 5 mm diameter and 15 mm length. The rotating disk speed was 0.5 ms^{-1}, under several nominal applied loads such as 50, 80, and 110 N which correspond to 2.54, 4.07, and 5.6 MPa nominal contact stresses for a established sliding distance of 3000 m. The pin samples were cleaned ultrasonically in acetone prior to each wear test. The specimens were weighted every 1000 m before and after each wear test by using a (GR200-AND) digital scale with an 0.1 mg accuracy. Weight loss and wear resistance (conversely ratio of weight loss per unit sliding distance m/mg), former versus sliding distance and latter versus applied load were plotted (look Figs. 5 and 6) so as to follow the variations very clearly.

Results and discussion

Microstructural evolution during isothermal aging

Figure 1a–d shows the microstructure of the as-cast and solution treated samples at 1230 °C for 3 h, respectively.

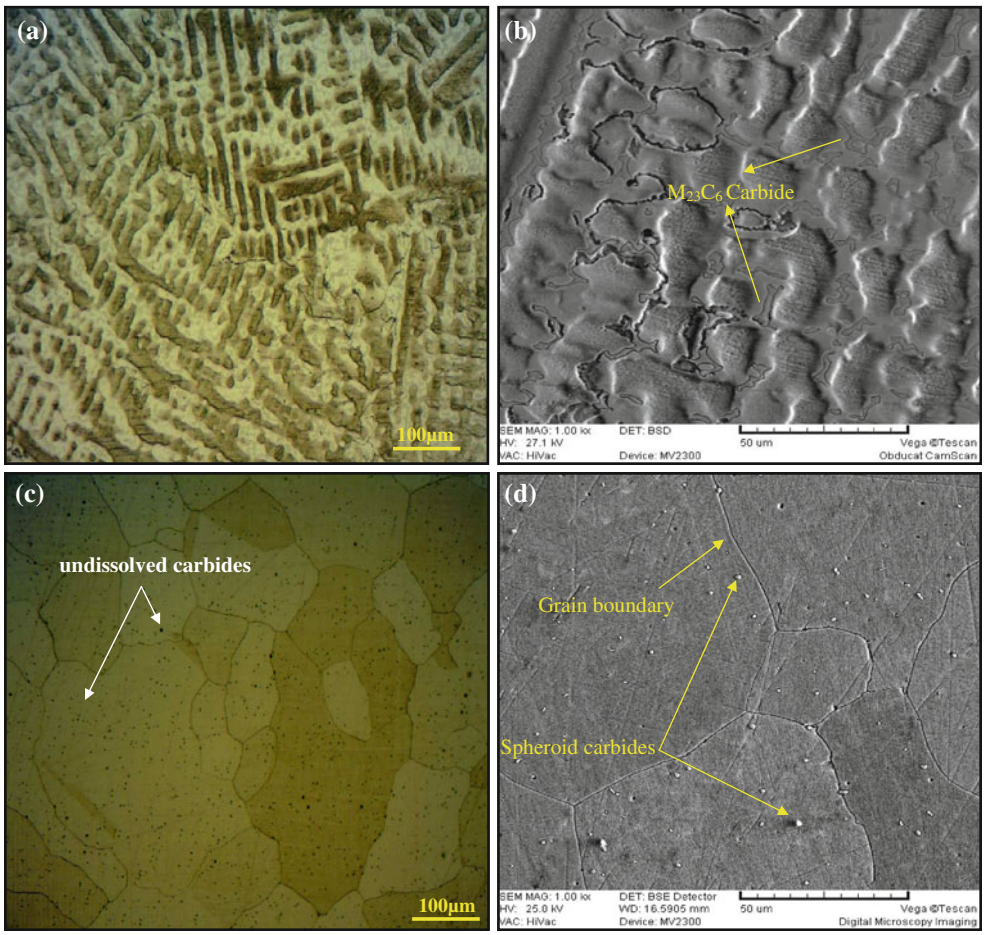

Fig. 1 Optical and SEM micrographs of **a** and **b** as-cast, showing primary carbides; **c** and **d** solutionized samples, showing undissolved carbides

In accordance with Fig. 1a, b, in as-cast specimen, coarse fcc dendrites and segregation of alloying elements particularly chromium in interdendritic regions, probably by the formation of $M_{23}C_6$ (M = Cr, Mo, Co), are observed. Several works available in the literature [4, 8, 9] have demonstrated that this dendritic microstructure can lead to poor properties and should be modified by the addition of alloying elements such as N, Zr, and etc. (as grain refiner), or by applying a suitable heat treatment process in order to obtain a uniform distribution of carbides within the microstructure. Concerning Fig. 1c, d, submitting solution treatment at 1230 °C for 3 h contributed to the elimination of primary grain boundary coarse Cr-rich carbides as well as coring (which are susceptible for cracking) and subsequently a fine and uniform distribution of primary $M_{23}C_6$ carbides in the cobalt-rich matrix was achieved. Figure 2a–d represents the microstructural evolution during isothermal aging at 850 °C for 4, 8, 16, and 24 h. As can be seen in these figures, a large amount of $M_{23}C_6$ carbides precipitated on the stacking faults (SFs) and lamellar-type carbides (γ-fcc + $M_{23}C_6$) at grain boundary zones are the concomitant results of aging times higher than 4 h. Regarding previous work [5, 6], it was observed that as aging time increases up to 16 h, the area fraction of lamellar-type carbides increases (from 3.7 ± 0.3 to 13 ± 0.9 wt pct), but at higher aging times (24 h), it decreases markedly ($\approx 7 \pm 1.2$ wt pct). Ramirez et al. [10] have shown that this lamellar component corresponds to a eutectoid constituent that precipitates below 989 °C in a Co–Cr–Mo–0.26C alloy, when cooling rate is below 35 °C/min.

Inasmuch as higher cooling rate was employed in this study, the formation of lamellar component was not observed after quenching, as can be seen in Fig. 1c, d. Isothermal aging of solution treated and quenched Co–28Cr–5Mo–0.3C alloy samples encourages the transformation of fcc → hcp (ε-martensite) by an intricate two-stage process, which happening synchronously with discontinuous reaction at the grain boundaries, resulting in a lamellar morphology [7]. During the early stages of aging, the hcp_1 phase is formed by a martensitic mechanism as a series of straight bands of heavily faulted whereas the hcp_2 phase, formed later during aging, shows a morphology including lamellar with a low faults density [7].

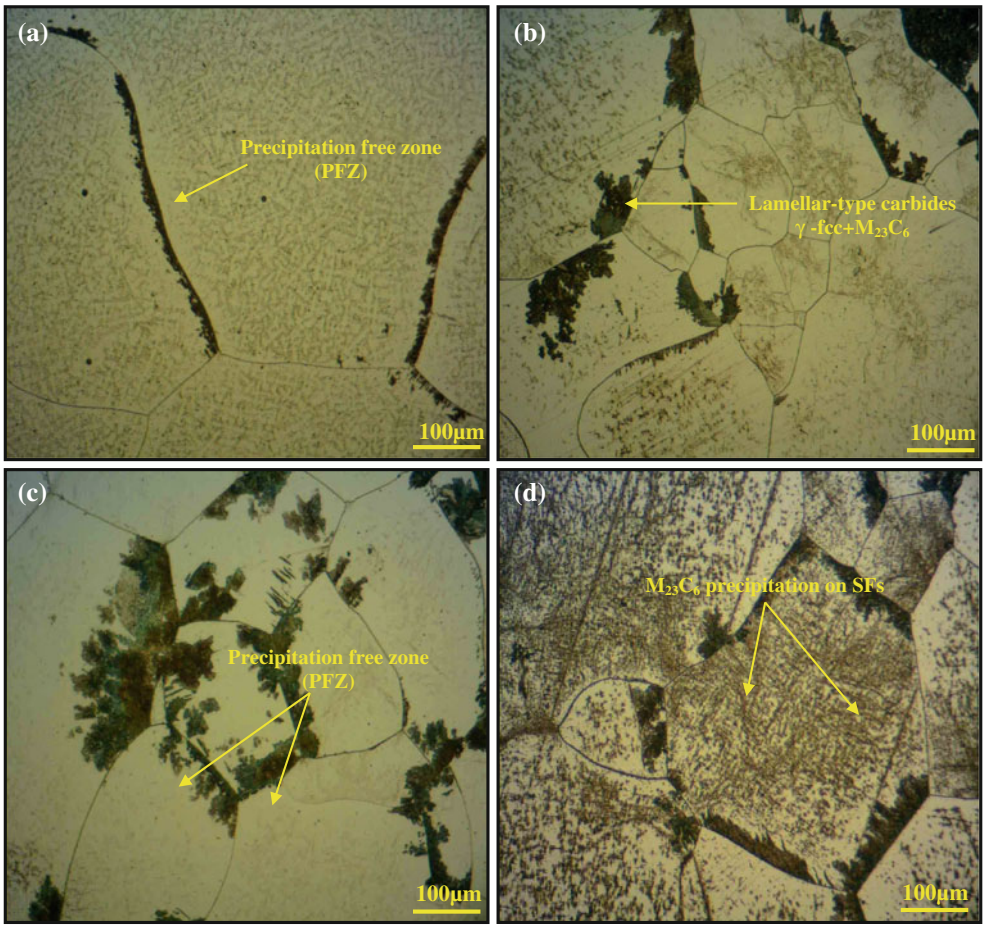

Fig. 2 Optical micrographs of isothermally aged specimens at 850 °C for: **a** 4 h, **b** 8 h, **c** 16 h, **d** 24 h, showing lamellar phases and PFZ

During isothermal aging of Co–28Cr–5Mo–0.3C alloy, metastable fcc phase transformed into hcp one. Figure 3a, b reveal back scatter SEM micrographs of the isothermally aged specimens at 850 °C for 16 h. As can be noticed, the lamellar phase nucleated at grain boundary regions and subsequently grew toward inside the grains. Besides lamellar-type carbides, it can be appreciated in Fig. 3a, b that some dark phases nucleated both as individual particles and within lamellar constituent, respectively. EDS point analysis of the dark phase was shown in Fig. 3c. According to literature [11, 12], this dark phases can be attributed to the σ phase. Moreover, it is worth noticing that the precipitation of those carbides in grain boundaries areas led to the formation of precipitation free zone (PFZ) at the adjacent of lamellar-type carbides noted in Fig. 2.

At higher aging time (24 h), large carbides precipitation within grain boundaries not only restricted the formation of lamellar-type carbides, probably due to reduction of chemical driving force for discontinuous reaction [5, 11], but also contributed to the higher microhardness values as compared with as-cast state specimen, Fig. 4 shows (where a 35% enhancement was achieved). In Fig. 5a–e, XRD patterns of solution treated and aged specimens are shown. It can be seen from this figure that the first $(111)_{fcc}$ and the second $(200)_{fcc}$ diffraction peaks of the fcc phase emerged at 2θ values of 43.65° and 50.97°, respectively. Moreover, for the hcp phase, the diffraction peaks of $(10\bar{1}0)_{hcp}$ $(0002)_{hcp}$ and $(10\bar{1}1)_{hcp}$ were located at 2θ values of 41.04°, 43.89°, and 46.93°, correspondingly. As indicated in Fig. 5, the relative intensities of the $(10\bar{1}0)_{hcp}$ and $(10\bar{1}1)_{hcp}$ diffraction peaks concurrently increase with increasing aging time at 850 °C. It would be expected a result of isothermal aging, the intensity of fcc peaks decreases while as shown in Fig. 5, it increases. These particular outcomes is in contrast with those obtained by Lopez et al. [13]. In their study, it seems that choosing lower solution temperature (1150 °C) and time (1 h) was not adequate to dissolve primary carbides. Therefore, during aging process the precipitation of carbides on stacking faults might not be significant. Nevertheless, in

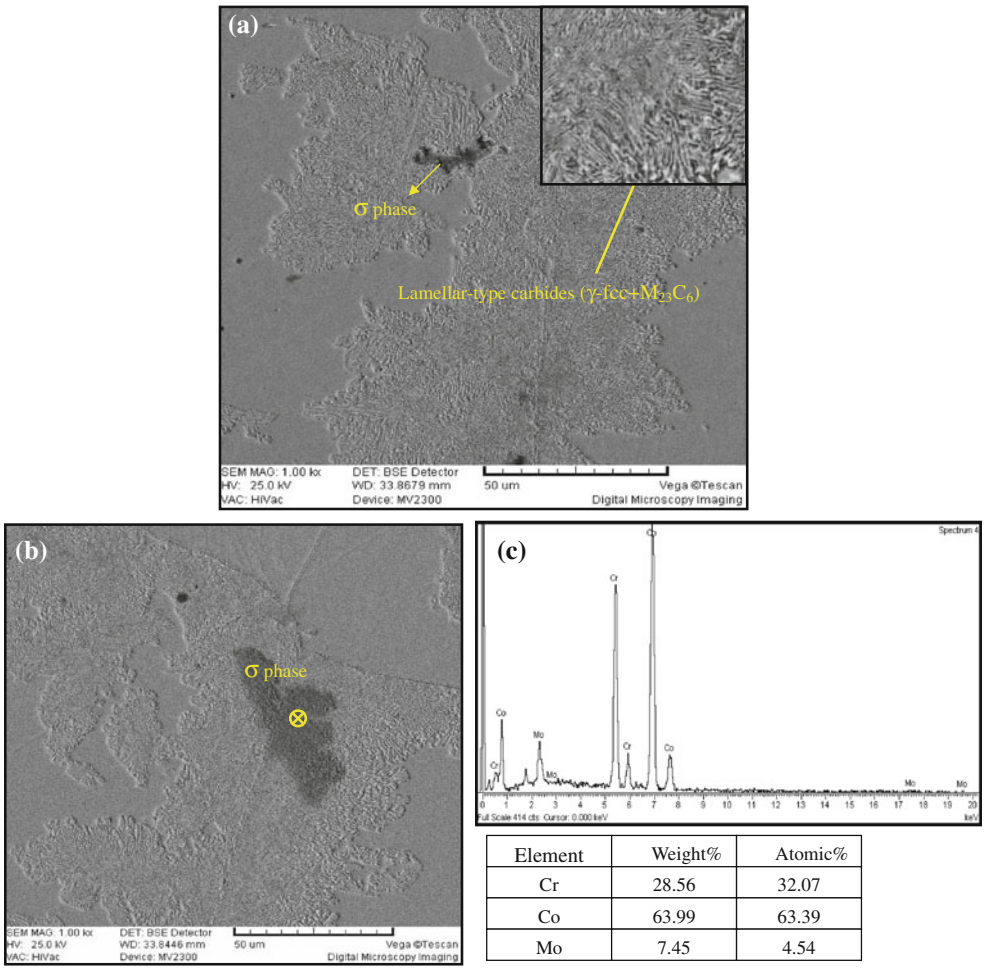

Element	Weight%	Atomic%
Cr	28.56	32.07
Co	63.99	63.39
Mo	7.45	4.54

Fig. 3 **a**, **b** SEM micrographs of 16 h isothermal aged specimens, showing lamellar-type constituent, **c** EDS analysis of and dark phase (probably σ phase)

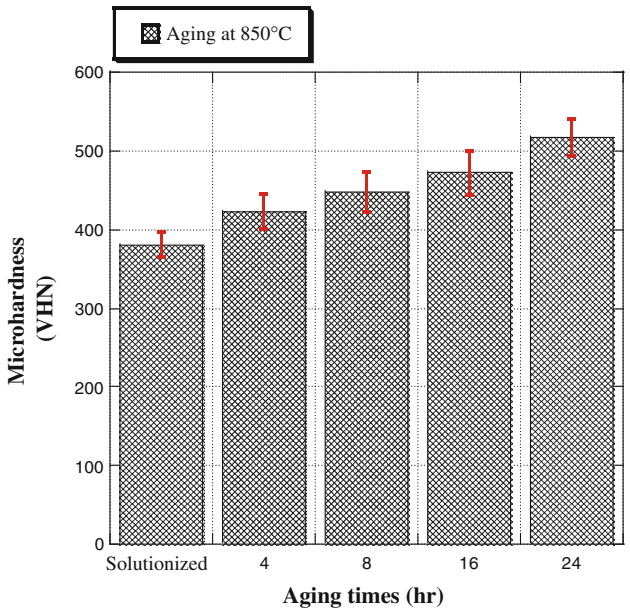

Fig. 4 Aging effect on the microhardness values

this study, presumably due to a higher solution temperature (1230 °C) and times (3 h), the dissolution of primary carbides was almost complete, Fig. 1c, d shows. Furthermore, due to closest matching of the (111) $M_{23}C_6$ and (111) fcc cobalt planes [11], the precipitation of secondary carbides occurred during isothermal aging might contribute to the increment of fcc diffraction peaks previously reported.

Isothermal aging effect on the dry sliding wear behavior of Co–28Cr–5Mo–0.3C alloy

Figure 6a–c shows the variation of weight loss as a function of sliding distance under different applied loads (50, 80, and 110 N) for both as cast and heat-treated samples. As can be seen in these figures, for the lowest applied load, isothermally aged specimens for 8 and 16 h show better wear properties when compared to as-cast as well as 4 and 24 h heat-treated specimens. On the other hand, as applied load increases from 50 N to 80 and 110 N, as-cast specimens indicate very suitable wear properties as compared to heat-treated specimens, since the wear behavior can be attributed to the different wear mechanism that acts in each loading condition.

It is worth considering the role of microstructural variation due to heat treatment process. As mentioned in literature [1, 3, 11], isothermally aging of Co–Cr–Mo–C alloys resulted in fcc → hcp phase transformation. This transformation during heat treatment occurs in order to reduce the stacking faults energy (SFE). Furthermore, besides to continuous precipitation of $M_{23}C_6$ carbides on the stacking faults within the grains, lamellar carbides (γ-fcc + $M_{23}C_6$) precipitated at the grain boundaries, as Fig. 2b–d shows. For the lowest load, it seems that aging process for 8 and 16 h contributed to the higher microhardness values due to carbide precipitation, as compared with as-cast specimen (where a 17 and 25% improvement was detected, respectively). In addition, applying heat treatment on as-cast samples, led to the uniform and homogenous dispersion of primary coarse carbides in the fcc matrix, as Fig. 2 indicates. In fact, preferential distributions of extensive interdendritic and coarse grain boundaries $M_{23}C_6$ carbides, as shown in Fig. 1a, significantly decrease the alloy ductility. This means that these coarse carbides can probably act as stress concentration regions and easy path to propagate cracks formed beneath the surface during wear sliding test. Therefore, higher microhardness and uniform distribution of secondary carbides after aging at 850 °C for 8 and 16 h might be the first reason for higher wear resistance of isothermally aged specimens when compared with as-cast specimen, as plotted in Fig. 7. Moreover, it is worthwhile to consider the role of lamellar-type carbide on the wear properties of the investigated alloy subjected under the applied load of 50 N. It is well-known that lamellar-type morphology have higher wear resistance as compared with spheroid carbides which can be attributed to the strong barrier against plastic deformation [14–16]. On the other side, in accordance with Fig. 2, it is interesting to note that as aging time proceeds up to 16 h,

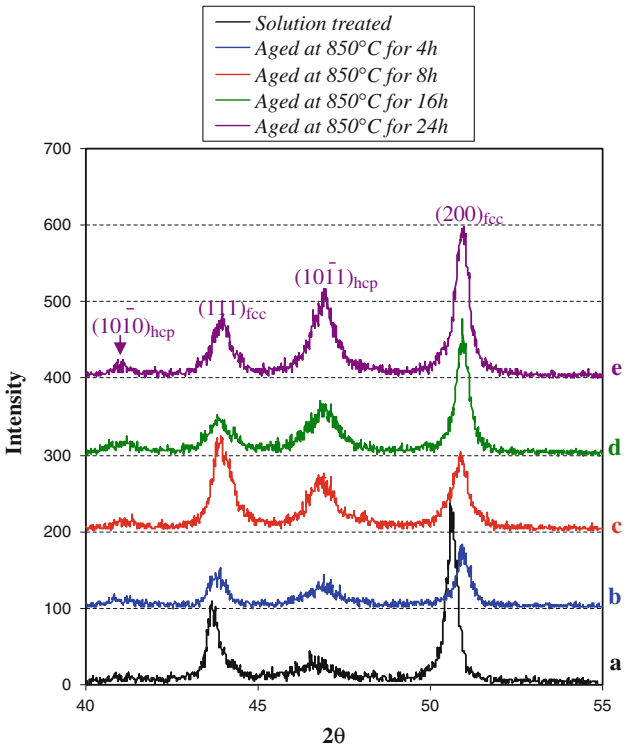

Fig. 5 XRD patterns of Co–28Cr–5Mo–0.3C alloy aged at 850 °C for: **a** solution treated state, **b** Aging for 4 h, **c** Aging for 8 h, **d** Aging for 16 h, and **e** Aging for 24 h

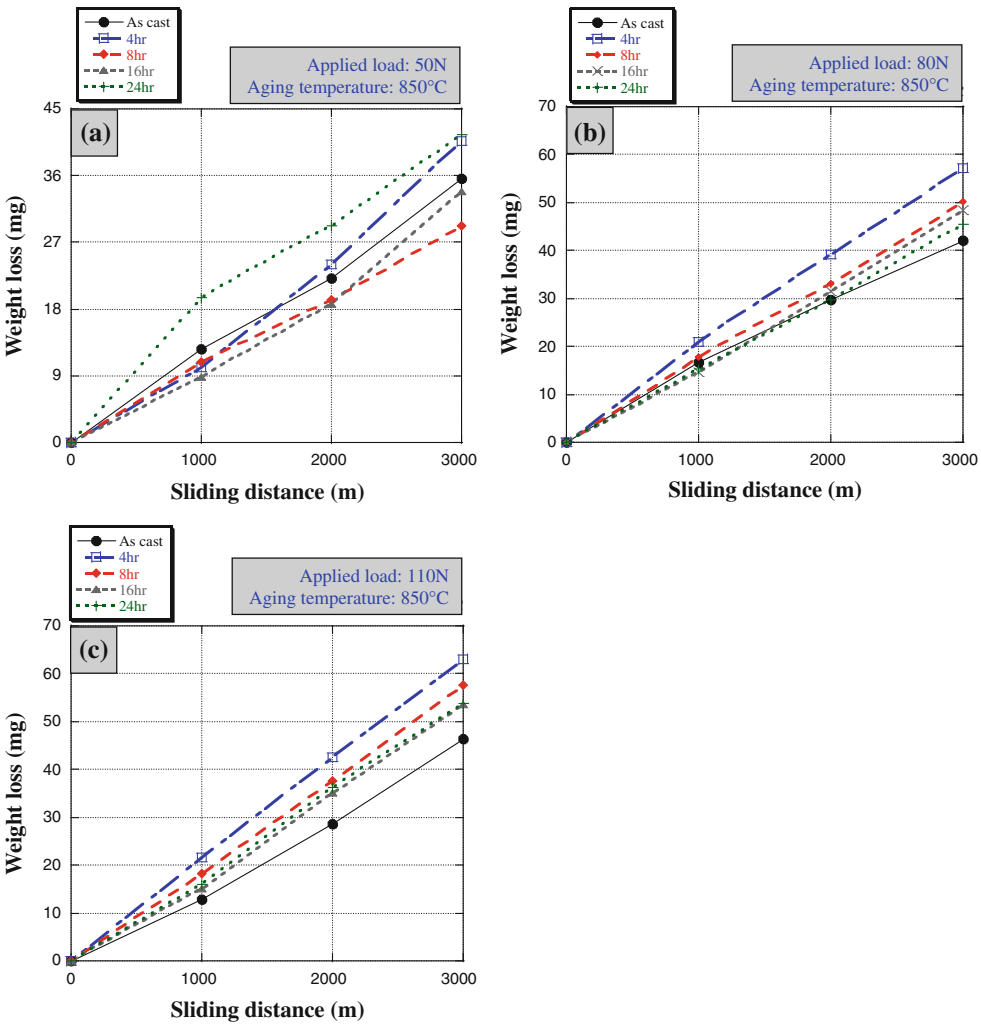

Fig. 6 Weight loss versus sliding distance for isothermally aged specimens at 850 °C for 4, 8, 16, and 24 h under nominal applied loads of: **a** 50 N, **b** 80 N, and **c** 110 N

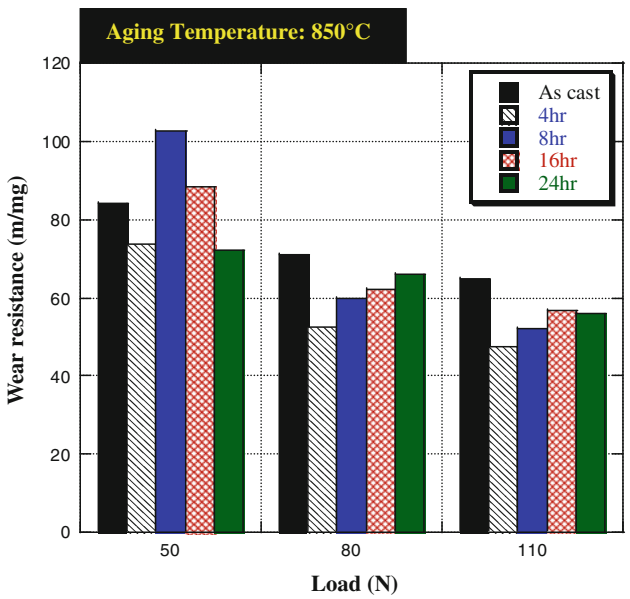

Fig. 7 Wear resistance as a function of applied load

area fraction of lamellar-type carbides increases and in higher aging time, i.e., 24 h, it decreases considerably. From Fig. 7, it can be concluded that for the lowest load (50 N), as lamellar-type carbides area fraction increases, the wear resistance enhances as well. On the other hand, the wear resistances of as-cast specimens were superior to heat treated specimens aged for lowest (4 h) and highest (24 h) aging time also shown in Fig. 7.

Concerning the Archard's equation law (1) expresses proportionality between the wear rate (Q), the applied normal load (W), and the hardness (H) of the wearing surface [14, 17], and also there is a converse relationship between the wear rate and hardness, as shown below:

$$Q = K \times \frac{W}{H} \tag{1}$$

where K is wear coefficient (Probability factor < 1), i.e., the fraction of contacts led to the formation of wear particles.

Regarding the aforementioned statement, it is expected higher wear resistance under 50 N applied load for 4 and

24 h isothermally aged specimens; for 4 and 24 h, however, the obtained results indicated different behavior. Isothermally aged specimens for lowest and highest aging time contributed to reduce the wear resistance which can be attributed to the microstructural variation during aging, as elucidated in following.

Although microhardness values for 24 h aged specimens improved more than a 35% as compared to as-cast specimens, but wear resistance decreased more than 10%. This behavior can be related to different microstructural features between isothermally aged specimens for 8 and 16 h and samples with 4 and 24 h, as shown in Fig. 2.

Elements such as Cr and Mo are believed to be hcp phase stabilizer in cobalt base alloys [1, 3, 5, 6, 17]. According to Fig. 2, large $M_{23}C_6$ carbide precipitation (M = Cr, Mo, Co) on the SFs within the grains which resulted in a depletion of chromium (Cr) and molybdenum (Mo) from matrix [5, 6] increasing the stacking fault energy [18]. It is very well-known that, dislocation cross-slip is usually hampered by the existence of stacking faults in fcc materials [18]. For this reason, as Cr and Mo (hcp phase stabilizer elements) contents decrease in the cobalt-base alloy matrix due to carbide precipitation, stacking fault energy increases. Higher stacking faults energy means that dislocation sliding would need less energy and would be relatively easy and of course a lower stress is needed for cross-slip. Figure 2a, d shows the severe precipitation of $M_{23}C_6$ (M = Co, Cr, Mo) carbides within the grain which can lead to depletion of matrix from Cr and Mo. As a result, wear resistance of isothermally aged specimens for 4 and 24 h is lower than for 8 and 16 h. Besides that, the absence of lamellar-type carbides in 4 and 24 h aging samples which can act as a strong barrier against sliding, could be another reason for the lower wear resistance for applied load of 50 N.

SEM micrographs of worn surfaces for 50 N load for isothermally aged specimens for 8 and 24 h are shown in Figs. 8 and 9, respectively. As can be seen in Fig. 8, the

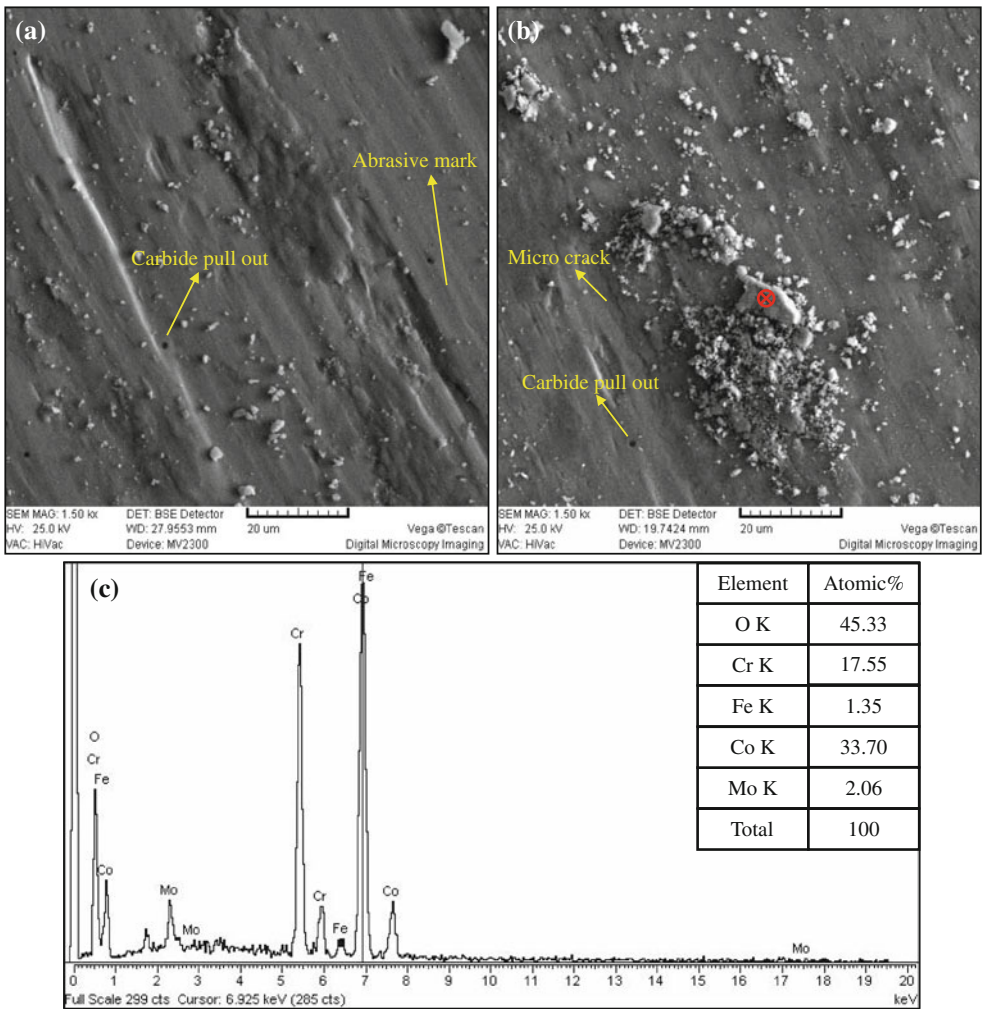

Element	Atomic%
O K	45.33
Cr K	17.55
Fe K	1.35
Co K	33.70
Mo K	2.06
Total	100

Fig. 8 **a**, **b** SEM micrographs of worn surface, and **c** EDS analysis of wear debris of aged specimen at 850 °C for 8 h at the applied load of 50 N

presence of abrasive marks, pits, and wear debris on the worn surface indicated that two and three-body abrasive wear mechanism were the dominant wear mechanisms for isothermally aged specimens. Furthermore, the fragments of broken carbides due to brittle fracture could also work as new abrasives; Fig. 8 shows abrasive tracks stemming from the fragmented carbides. In addition, some pits were observed on the worn surface indicating that the carbides were pulled out. Also, some microcracks were observed on the worn surfaces of isothermally aged specimen for 8 h; however, they were not very significant. In accordance with Fig. 8b, the formation of debris fragments which are observable over the worn surface, is due to asperity interaction (probably multiple occurrences within a contact) led to junction formation, deformation and fracture. Owing to the joint failure or fracture, materials immediately are transferred to the counter face adhesively, so as to form a new asperity on the worn surface. Further sliding results in more fragments to be formed, to which adhere the original fragment until a much larger conglomerate wear debris finally becomes detached [14, 17]. As can be seen in Fig. 8b, these debris on the worn surface, which can act as extra abrasive agents in a three-body wear mechanism, was found to be roughly equiaxed. In Fig. 8c, the EDS analysis of the fragmented debris shows the complex $Co_xCr_yO_z$ compound (probably $CoCr_2O_4$) and iron oxide particles on the worn surface. As mentioned earlier, when aging time reaches 24 h, owing to significant microstructural changes, the wear behavior varied as well, this behavior can be observed in Figs. 2 and 7. SEM micrographs of the worn surface for a 50 N load and 24 h isothermally aged specimen are shown in Fig. 9a, b. Moreover, for a better understanding of the wear behavior, the study of wear debris is also essential. In Fig. 10a–c, SEM micrographs of worn debris for both as-cast and 24 h isothermally aged specimen are also presented. In accordance with these figures, delamination wear mechanism seems to be the dominant wear mechanism. This mechanism involves nucleation and an ulterior propagation of subsurface cracks parallel to the surface [14]. The cracks initiate due to plastic deformation occurring beneath the surface probably but not necessarily from voids, also brittle or coarse carbides; weak bonding between carbides and the cobalt-rich matrix can also act as preferential sites for crack initiation caused by the shearing of inclusions. Finally, microvoids after growing and linking together, reach the sliding surface which is noticed in Figs. 9 and 10c show flake-like debris which are concurrent results of detachment. The wear debris of as-cast specimen at different magnifications, is shown in Fig. 10a, b would suggest that the surfaces under nominal applied load of 50 N were oxidized and then compacted in the close contact between two surfaces in order to form a tribolayer. Subsequently, the deformation of this layer led to the delamination and eventually fracture of oxide film on the worn surface and to the formation of wear debris. As mentioned in the literature [14, 17, 19], that critical load, W^*, is needed to nucleate the lateral crack. Therefore, if the applied load is high enough to exceed a critical load, cracks will nucleate. Therefore, the onset of cracks relies on the fracture toughness of the alloy, K_{IC}, and on its hardness, H, as follows [19]:

$$W^* \alpha K_{IC}^4 / H^3 \tag{2}$$

As mentioned earlier, the isothermally aging heat treatment at 850 °C for 24 h led to a 35% increase increment in the microhardness. According to Eq. 2, an increase of 1/3 on the hardness value causes W^* to decrease up to 1/9. Probably due to this reason, isothermally aged specimen at 850 °C for 24 h with heavy precipitation of carbides on SFs shows lower wear resistance as compared with as-cast and isothermally aged specimen for 4, 8, and 16 h.

At higher applied loads, such as 80 and 110 N, the dry sliding wear behavior of as-cast specimens seem to be much better in comparison with all heat treated samples, as

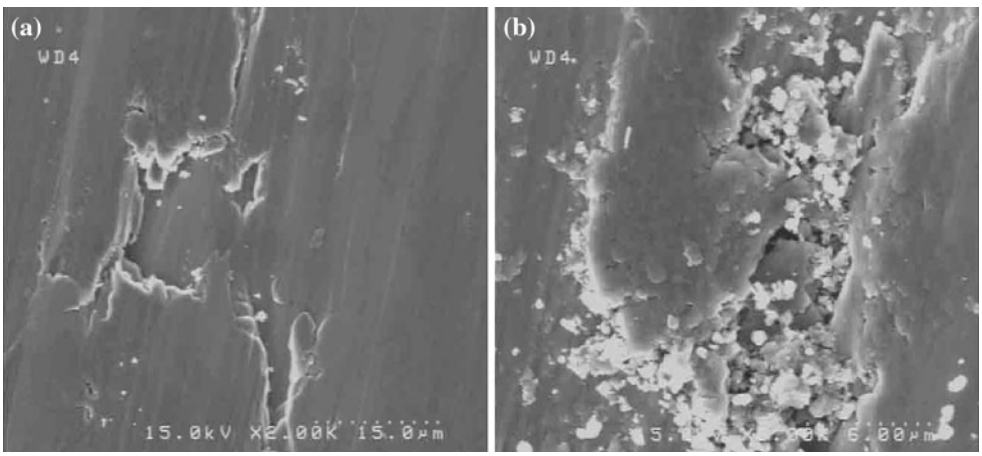

Fig. 9 SEM micrographs of worn surfaces of aged specimen at 850 °C for 24 h at the applied load of 50 N

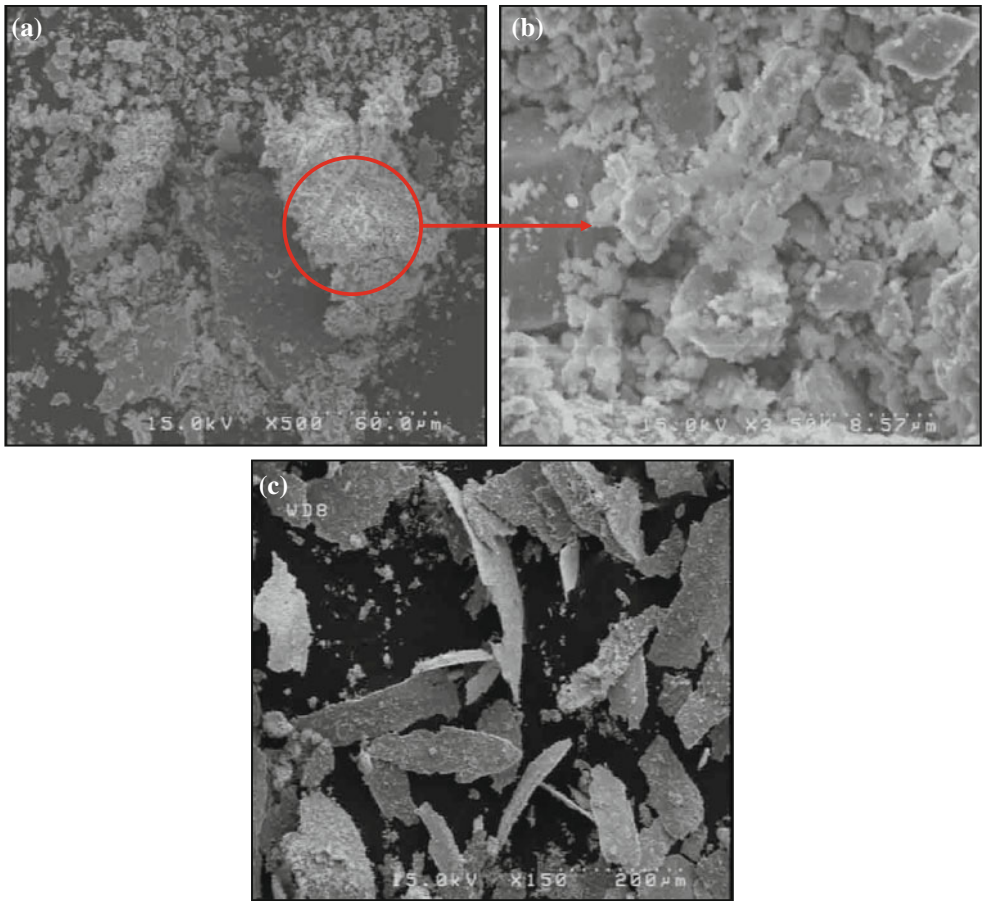

Fig. 10 SEM micrograph of debris particles under an applied load of 50 N: **a**, **b** As-cast specimen, **c** 850 °C for 24 h

Figs. 6 and 7 show. The rate of heat generated per unit of contact [14], $Q^{\bullet}$, is calculated as follows (3):

$$Q^{\bullet} = \mu WV \tag{3}$$

where μ is the friction coefficient, W is the contact stress, and V is the relative sliding speed.

According to the Eq. 3, once the contact stress increases by increasing the load applied during sliding tests at room temperature, significant oxidation occurs at contact asperities. Inasmuch as no inert gas was used to separate the contact surfaces against air, it is reasonable to expect that oxygen ions can diffuse inward and, metal ions can diffuse outward in order to interact with each other to form a tribolayer, also known as mechanically mixed layer (MML) [17]. In fact, this strong increment of oxidation by sliding might result from increased diffusion rates of ions thorough a growing oxide layer which has high defect content (e.g., voids, dislocations, and vacancies) owing to mechanical perturbation. Once oxide films reach a critical thickness, they become unstable and breaks up to form flake-like debris.

In this study, the obtained results showed that by increasing the load applied from 50 to 110 N, the wear rate in all specimens decreased as Fig. 7 shows. This transition from severe to slight wear can be attributed to the formation of an oxide layer or tribolayer which can act as a solid lubrication agent to separate the worn surfaces from each other [14, 17, 20, 21].

SEM micrographs of worn surfaces and debris for as-cast specimens for 80 and 110 N loads are shown in Figs. 11 and 12. In these figures, the presence of oxide layer on the worn surface and bright debris particles scattered on the worn surface, corroborate the wear mechanism proposed for higher loads. Moreover, due to the long sliding distance (selected for conducting the tests 3000 m) and high imposed load (110 N), the fragmented flake-like debris can be flattened and elongated in the sliding direction by further plastic deformation, as shown in Fig. 11b. By increasing loads from 80 to 110 N in as-cast specimens, worn debris morphology varies from compacted oxide to flake-like, as Fig. 11a–d shows. In fact, the plastic deformation of oxide layer contributed to the delamination and

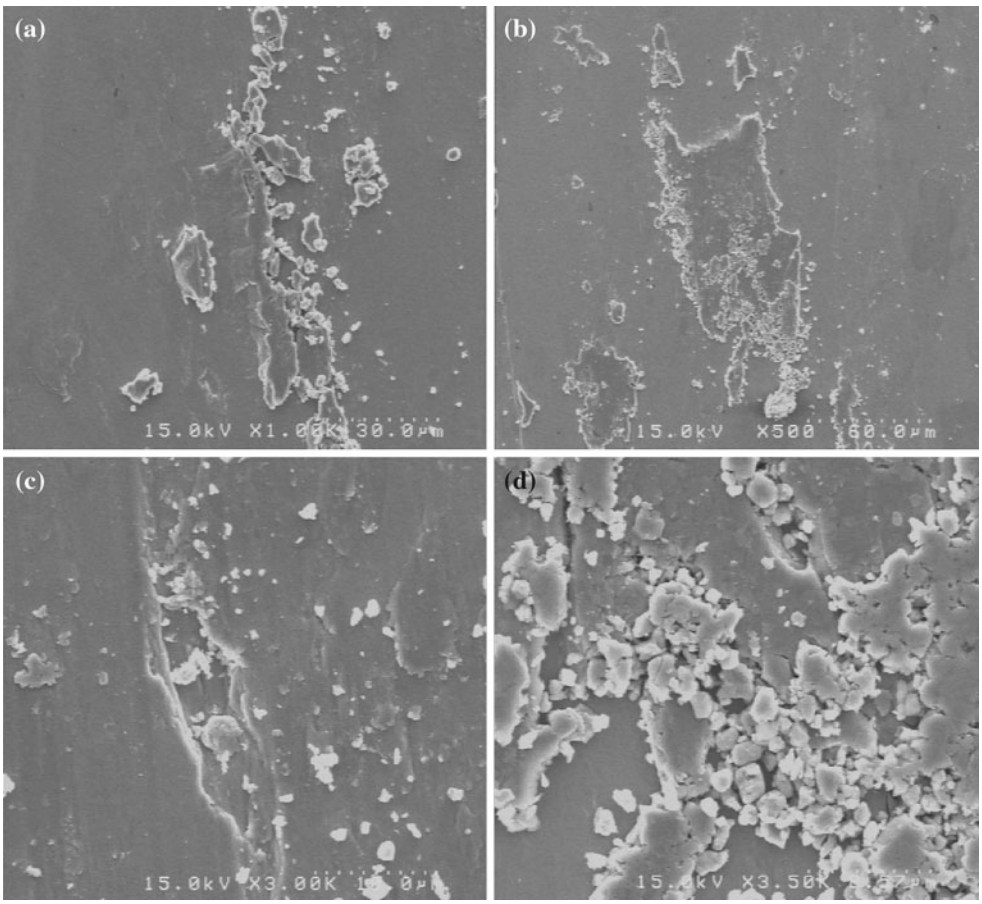

Fig. 11 SEM micrograph of worn surfaces of as-cast specimens under an applied load of 110 N

fracture of oxide film and eventually generation of flake-like debris.

Even though, by increasing the applied load from 50 N to 80 and 110 N, the wear rate decreases significantly due to the formation of an oxide layer over the worn surface, it is noteworthy that at higher loads, like 80 and 110 N, the as-cast specimens show higher wear resistance as compared to heat treated samples for various times, shown in Fig. 6.

To determine the reason why the as-cast specimens wear resistance is higher than all heat treated samples, it seems to be essential to consider the nature of the oxide compounds formed during sliding tests. Clemow and Daniell [20], indicated that CoO, $CoCr_2O_4$, and Co_3O_4 are the main oxide compounds arising from sliding wear of the as-cast samples. In their study, the heat treatment conducted contributed to the formation of an Chromium-oxide compound on the worn surface. It is well-known that, the nature of oxide adhesion on the worn surface varies depending in the oxide nature. This means that due to porous morphology of Cr_2O_3, the bonding between this oxide and a sub layer is not very strong and this reduces the adhesion of oxide layer on Co–Cr alloys [20].

Figure 13a–d is the SEM micrograph and EDS analysis of isothermally aged specimen for 4 h under 110 N testing load, indicating the generation of chromium-oxide compound identified as the slightly dark phase in Fig. 13a, b and a cobalt oxide compound identified as the bright phase in Fig. 13c, d. It seems that chromium concentration during isothermal aging process varied across the microstructure due to the precipitation of $M_{23}C_6$ carbides. This variation probably resulted in the subsequent formation of Cr_2O_3 compound at the metal/oxide interface which can cause to the lesser oxide adhesion, and higher weight loss in all heat treated specimens. In the as-cast alloy, however, inter-dendritic regions contain higher equilibrium Cr concentration and therefore would be expected to behave similarly to heat treated samples; although due to the different oxidation rates between the dendritic and interdendritic regions with higher oxidation rate of dendrites which are enriched in Co as compared to interdenritic regions which are Cr-rich [20], as-cast samples showed higher wear resistance in comparison with heat treated specimens at higher loads such as 80 and 110 N. This means that, dendritic regions will oxidate faster and finally the adhesive

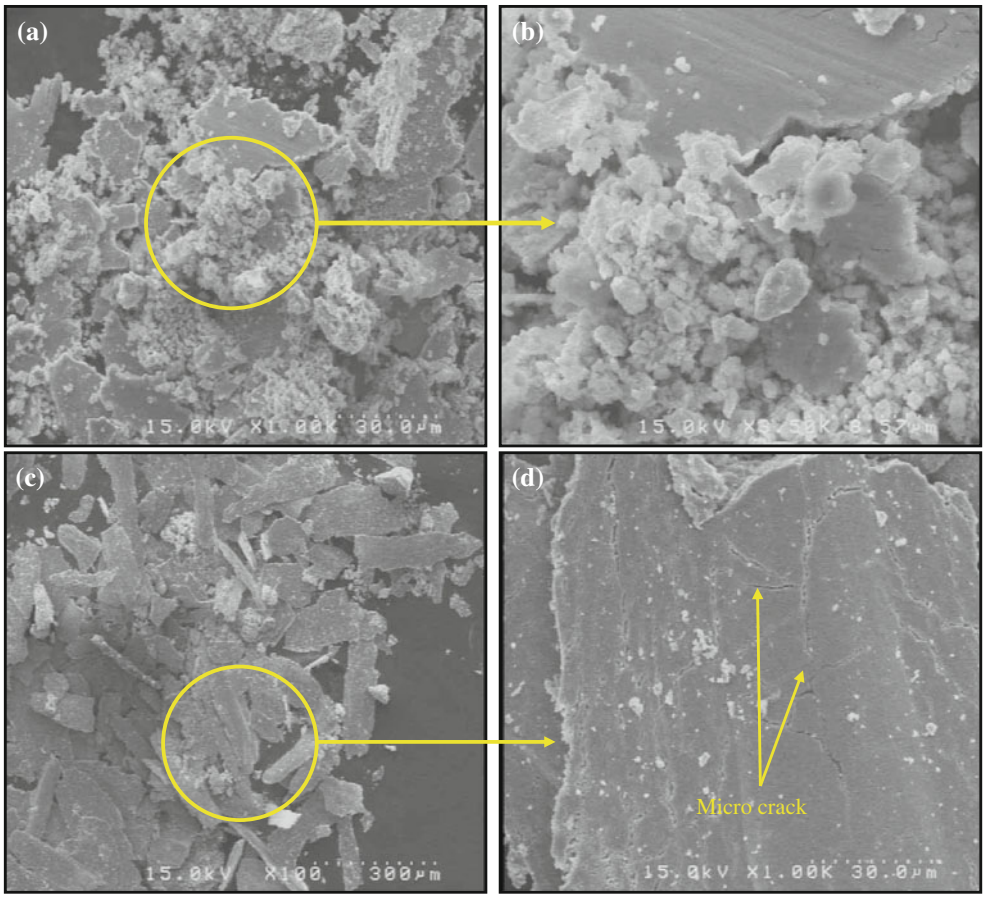

Fig. 12 SEM micrograph of as-cast debris under an applied loads of: **a**, **b** 80 N and **c**, **d** 110 N

cobalt oxide compounds formation on the worn surface would have a tendency to generate higher wear resistance when compared with aged specimens for higher loads.

Table 2 shows the wear factors calculated from experimental data for the as-cast and heat treated specimens at different loads. The wear factor, k, was determined by dividing the average wear rate by the normal applied load [14, 17, 21]. From the data reported in Table 2, it can be concluded that, probability of the debris formation is smaller in as-cast specimens at higher loads which can be related to the strong bonding between the oxide layer and sub surface when compared with heat treated samples.

Figure 14a, b shows the longitudinal cross-section area of as-cast and isothermally aged specimen at 850 °C for 24 h, respectively, both subjected to a 110 N load. It can be noticed that, due to highly deformation of the subsurface layer, $M_{23}C_6$ carbides were fragmented and aligned toward the sliding direction. The fragmented carbides, shown in Fig. 14b, can reach the surface due to wear and subsequently mixed with the oxides in the contact area so as to form a tribolayer known as mechanically be mixed layer. The presence of fragmented carbides could weaken the tribolayer stability and finally facilitate the nucleation and propagation of microcracks in the tribolayer due to their poor bonding in the tribolayer, as Fig. 14a shows.

Conclusions

The main conclusions to be drawn from the discussion are as follows:

(1) Isothermally aging at 850 °C for more than 4 h contributed to the formation of this lamellar-type carbides (γ-fcc + $M_{23}C_6$) at the grain boundaries. The area fraction of lamellar phase increased up to 16 h aging and then decreased drastically as aging time progresses.
(2) At the lowest load applied (50 N), owing to fine dispersion of $M_{23}C_6$ and lamellar-type carbides, wear resistance of isothermally aged specimens for 8 and 16 h was found to be higher than as-cast and heat treated specimens for 4 and 24 h aging times.
(3) For higher applied loads (80 and 110 N), due to the formation of adhesive cobalt oxide compound on the

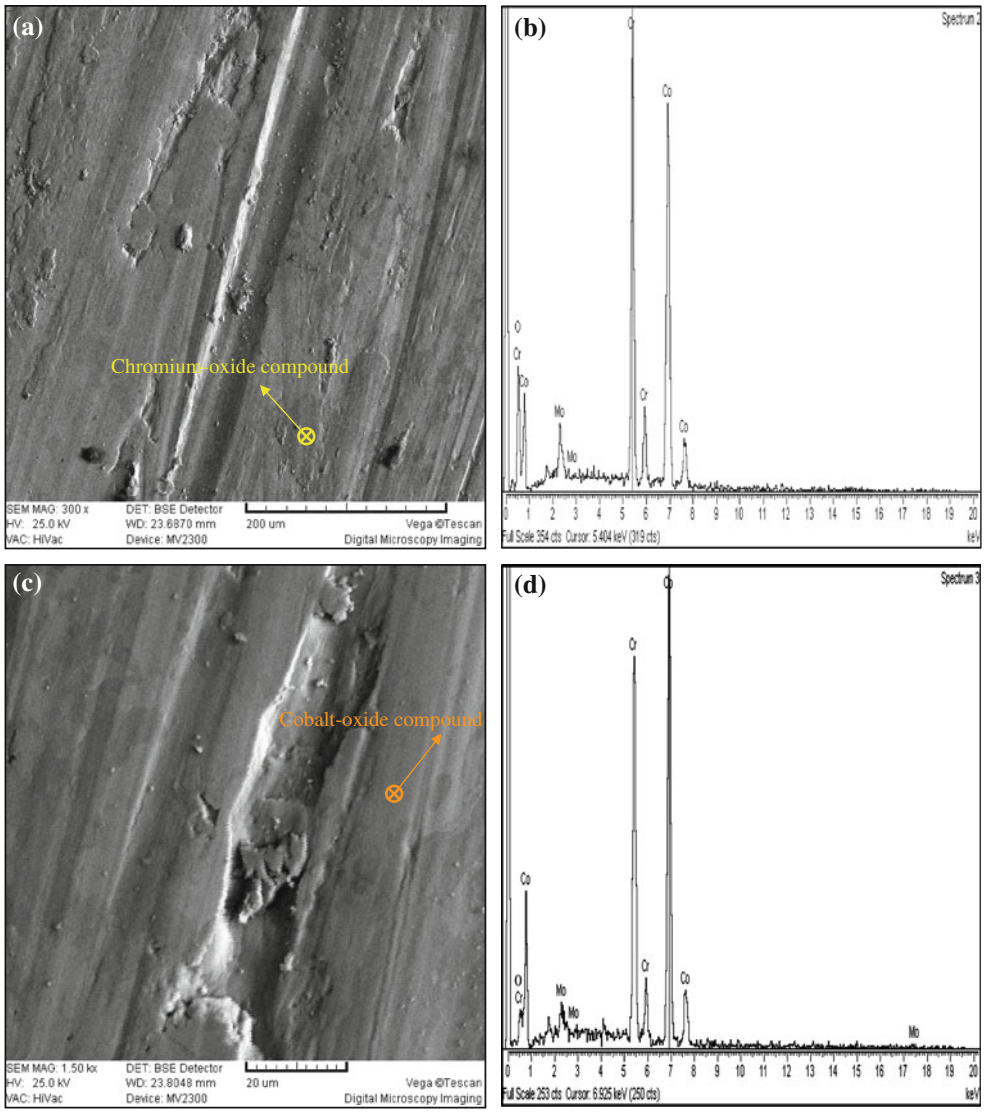

Fig. 13 SEM micrographs and EDS analysis of worn surfaces of 4 h aged samples for the load of 110 N, **a**, **b** showing Chromium-oxide compound (*slightly dark phase*), **c**, **d** showing Cobalt-oxide compound (*bright phase*)

Table 2 Wear coefficient (10^{-4} mg m^{-1} N^{-1}) function of heat treatment time with different loads applied

Samples	Loads		
	50 N	80 N	110 N
As-cast	2.373	1.758	1.406
Aged at 850 °C for 4 h	2.706	2.379	1.912
Aged at 850 °C for 8 h	1.946	2.091	1.748
Aged at 850 °C for 16 h	2.26	2.012	1.621
Aged at 850 °C for 24 h	2.766	1.891	1.627

worn surface of as-cast specimens, wear resistance increased when compared to all heat treated samples.

(4) Under lower applied load, two and three-body abrasive wear mechanism both were the dominant wear mechanisms whereas at higher loads oxidation

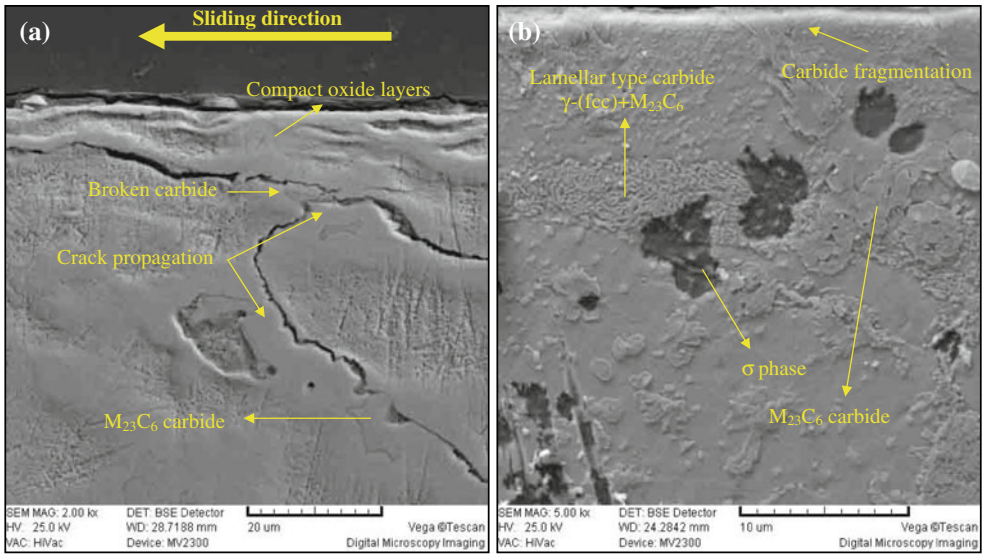

Fig. 14 Side views of the worn pin samples under an applied load of 110 N: **a** as-cast, **b** 850 °C for 24 h

and delamination of oxide layer were found to be the dominant wear mechanisms.

(5) In all the specimens under study, the generation of oxide layer on the worn surface can act as a solid lubricant and finally lead to reduction wear rate.

Acknowledgement H. R. Lashgari wishes to acknowledge the assistance of Mr. Saghafi for operating SEM in this project.

References

1. Saldivar AJ, Lopez HF (2001) Scr Mater 45:427
2. Upadhyay D, Panchal MA, Dubey RS, Srivastava VK (2006) Mater Sci Eng A 432:1
3. Huang P, Lopez HF (1999) Mater Lett 39:249
4. Montero-Ocampo C, Talavera M, Lopez HF (1999) Metall Mater Trans A 30:611
5. Lashgari HR, Zangeneh Sh, Hasanabadi F, Saghafi M (2010) Mater Sci Eng A 527:4082
6. Zangeneh Sh, Lashgari HR, Saghafi M, Karshenas M (2010) Mater Sci Eng A 527:6494
7. Garcia A, Medrano A, Rodriguez A (1999) Metall Mater Trans 30:1177
8. Garza Z, Herrera-Trejo M, Castro M, Ramırez E, Méndez M, Méndez J (2001) J Mater Eng Perf 10:153
9. Escobedo J, Mendez J, Cortes D, Gomez J, Mendez M, Mancha H (1996) Mater Des 17:79
10. Ramırez-Vidaurri LE, Castro-Roman M, Herrera-Trejo M, Garcia-Lopez CV, Almanza-Casas E (2009) J Mater Proc Technol 209:1681
11. Taylor RNJ, Waterhouse RB (1983) J Mater Sci 18:3265. doi: 10.1007/BF00544151
12. Giacchi JV, Morando CN, Fornaro O, Palacio HA (2011) Mater Charact 62:52
13. Lopez HF, Saldivar-Garcia AJ (2008) Metall Mater Trans A 39:8
14. ASM Handbook (1992) In: Friction, lubrication, and wear technology, vol. 18. ASM International, Hardcover
15. Ueda M, Uchino K, Kobayashi A (2002) Wear 253:107
16. Clayton P (1980) Wear 60:75
17. Bhushan B (ed) (2001) In: Modern tribology handbook, vol. 1. CRC press LLC, Boca Raton
18. Bhansali KJ, Miller AE (1982) Wear 75:241
19. Yu H, Ahmed R, Lovelock HV, Davies S (2009) J Tribo 131:11601
20. Clemow AJT, Daniell BL (1980) Wear 61:219
21. Haung P, Rodriguez AS, Lopez HF (1999) Mater Sci Tech 15:1324